Click Here for Full Article

Influence of soil water content on the thermal infrared emissivity of bare soils: Implication for land surface temperature determination

M. Mira,[1] E. Valor,[1] R. Boluda,[2] V. Caselles,[1] and C. Coll[1]

[1]   The influence of soil water content in thermal infrared emissivity is a known fact but has been poorly studied in the past. A laboratory study for quantifying the dependence of emissivity on soil moisture was carried out. Six samples of surface horizons of different soil types were selected for the experiment. The gravimetric method was chosen for determining the soil moisture, whereas the emissivity was measured at different soil water contents using the two-lid variant of the box method. As a result, the study showed that emissivity increases from 1.7% to 16% when water content becomes higher, especially in sandy soils in the 8.2–9.2 μm range. Accordingly, a set of equations was derived to obtain emissivity from soil moisture at different spectral bands for the analyzed mineral soils. Moreover, results showed that the spectral ratio decreases with increasing soil water content. Finally, the study showed that systematic errors from 0.1 to 2 K can be caused by soil moisture influence on emissivity.

Citation: Mira, M., E. Valor, R. Boluda, V. Caselles, and C. Coll (2007), Influence of soil water content on the thermal infrared emissivity of bare soils: Implication for land surface temperature determination, *J. Geophys. Res.*, *112*, F04003, doi:10.1029/2007JF000749.

1.   Introduction

[2]   The emissivity of natural surfaces is a magnitude required for the determination of land surface temperature (LST) from thermal infrared (TIR) radiance measurements. If the emissivity is not well determined, it can cause a significant error in obtaining LST. For this reason, it is necessary to study the factors that influence emissivity, since it must be estimated with the highest possible accuracy.

[3]   The soil type influence on emissivity is well known from experimental studies [*Salisbury and D'Aria*, 1992a]. However, the analysis of the variation of TIR emissivity with soil moisture (SM) is one of the pending issues in thermal remote sensing. The SM dependence should be taken into account in emissivity retrievals from satellite data observations, since the SM variation may cause a high systematic error in this parameter, e.g., about +0.1 in emissivity for an increase from 0.04 to 0.10 g/cm^3 in SM for sandy soils [*Ogawa et al.*, 2006].

[4]   At microwave wavelengths there are several theoretical [*Galantowicz et al.*, 2000] and also experimental studies [*Alex and Behari*, 1998; *Jackson et al.*, 1999; *Burke and Simmonds*, 2003] about the emissivity variation with SM. In this region, this variation is much more significant than in the thermal infrared. The microwave emissivity measurements by passive radiometry are, in fact, the basis of one of the synoptic measurement methods of SM in remote sensing [*Simmonds et al.*, 2004].

[5]   Few studies concerning this topic have been published in the TIR, mainly in the experimental domain. *Van Bavel and Hillel* [1976] reported that emissivity significantly increases with soil water content, and *Chen et al.* [1989] showed that it should also depend on soil surface structure, with this increase being more apparent in compacted soils ($\varepsilon = 0.915 + 0.052\Theta_v$; R^2 = 0.99; where Θ_v is the volumetric water content) than in tilled ones ($\varepsilon = 0.937 + 0.019\Theta_v$; R^2 = 0.95). *Salisbury and D'Aria* [1992b] noted that as the weight percent of soil moisture increases from air-dried soil to 7%, the emissivity increases by about 5% in the 8–9 μm region. By means of the analysis of Advanced Spaceborne Thermal Emission and Reflection Radiometer (ASTER) 10/14 {8.3 μm/11.3 μm} reflectance ratio, it was shown that this spectral ratio decrease was linear with increasing moisture content. Dry sand with large amounts of quartz and feldspar was used by *Urai et al.* [1997] to show that the emissivity ratio of averaged ASTER TIR channels (10, 11, 12)/(13, 14), {8–9.5 μm}/{10–12 μm}, increases by about 3% with increase in SM content from 0 to 2% in weight. The results showed an emissivity increase with SM in the 8–10 μm range, and no changes were observed in the 11–13 μm range. More recently, a dependence of emissivity on sand content was observed by *Xiao et al.* [2003], in the way that emissivity becomes higher when sand content decreases and water content increases in 8 μm and 9.5 μm bands, whereas the variance of emissivity is not obvious in channels placed at 11 μm and

---

[1]Department of Earth Physics and Thermodynamics, Faculty of Physics, University of Valencia, Burjassot, Spain.

[2]Department of Vegetal Biology, Faculty of Pharmacy, University of Valencia, Burjassot, Spain.

Table 1. Physical and Chemical Soil Sample Properties, Followed by Their Taxonomic Class, Diagnostic Horizon and Origin, as Well as Their Mineral Composition and Bulk Density and Field Capacity[a]

	Samples					
	A	B	C	D	E	F
Color, dry	5YR4/6	10YR8/1	10YR4/2	10YR6/2	10YR5/6	10YR5/4
Color, wet	7.5YR3/4	10YR7/2	10YR2/2	2.5Y4/2	10YR3/3	10YR5/3
pH (H_2O) 1:2.5	7.50 ± 0.04	9.28 ± 0.06	7.50 ± 0.10	7.7 ± 0.4	5.18 ± 0.01	8.2 ± 0.2
pH (KCl) 1:2.5	6.9 ± 0.3	8.79 ± 0.04	6.70 ± 0.07	7.1 ± 0.4	4.46 ± 0.01	7.70 ± 0.10
EC 1:5 (dS/m)	0.40 ± 0.12	0.04 ± 0.01	0.48 ± 0.10	0.58 ± 0.09	0.15 ± 0.01	0.2 ± 0.3
OM, %	2.1 ± 0.3	<0.1	8.9 ± 0.5	4.5 ± 0.4	1.5 ± 0.1	3.5 ± 0.4
$CaCO_3$, %	1.7 ± 0.1	<0.1	23.6 ± 2.9	44 ± 6	0	46 ± 8
CEC, $cmol_c\ kg^{-1}$	21.3 ± 1.7	0.0	34.6 ± 3.5	24 ± 3	9.8 ± 1.9	14.7 ± 1.4
V, %	100	0	100	100	59 ± 6	100
Sand, %	41 ± 3	99 ± 6	20 ± 1	14 ± 6	67 ± 4	50 ± 3
Silt, %	28 ± 1	1 ± 1	43 ± 2	50 ± 8	20 ± 1	30 ± 2
Clay, %	31 ± 2	0 ± 0	37 ± 3	35 ± 4	13 ± 1	20 ± 1
Texture (USDA)	clay loam	sand	silty clay loam	silty clay loam	sandy loam	loam
Soil taxonomy [*FAO*, 1999]	luvic Calcisol	albic Arenosol	calcic Kastanozem	gleyic-calcaric Fluvisol	dystric Cambisol	petric Calcisol
Soil taxonomy [*Natural Resources Conservation Service*, 1999]	rhodoxeralf	xeropsamment	calcixeroll	fluvaquent	dystrudept	petrocalcid
Diagnostic horizon	irragric	antropic	mollic	antraquic	cambic	ocric
Sample origin in Spain	a citrus orchard, Valencia	a quarry, Valencia	Las Nogueras, Valencia	Albufera, Valencia	A Coruña	Camporrobles, Valencia
Quartz, %	82.0	95.3	29.4	19.3	72.0	19.9
Feldspar, %	5.2	2.9	5.5	3.5	21.4	4.5
Filosilicate, %	5.0	-	9.0	6.0	3.2	4.1
Calcite, %	2.9	-	56.1	62.3	-	62.9
Hematite, %	4.9	-	-	8.9	-	8.7
Bulk density, $10^3 \times kg/m^3$	1.34	2.09	0.90	1.27	1.52	1.43
Field capacity, $kg\ kg^{-1} \cdot 100$	22.1	3.8	-	28.3	13.2	17.5

[a]Bulk density and field capacity values were calculated according to *Saxton et al.* [1986], taking into account the soil texture. An exception was bulk density of sample C, which was obtained experimentally according to *Soriano and Pons* [2001] because of its high organic matter content, which is not considered by the method of Saxton et al. EC., electric conductivity; OM, organic matter; CEC, cationic exchange capacity; V, base saturation.

13 μm. Finally, *Ogawa et al.* [2006] have recently published the emissivity variations in several sites over North Africa and the Arabian Peninsula, where they found no correspondence with the Normalized Difference Vegetation Index, NDVI (derived from Moderate Resolution Imaging Spectroradiometer, MODIS), whereas the TIR emissivity increase was found to be qualitatively correlated with an increase in Advanced Microwave Scanning Radiometer (AMSR) derived SM in some regions.

[6] As seen above, the emissivity variation with SM has not been fully evaluated. Some observations mainly for sand with large amounts of quartz and feldspar have always been the object of these studies, since it is the kind of soil that shows the highest emissivity variation with SM. It is the purpose of this paper to fill this gap to some extent by analysing the emissivity variation with SM for a variety of bare soils. This study will allow us to estimate more accurate emissivity values from space using the SM estimates, provided by future sensors such as the MIRAS instrument of the ESA's Soil Moisture and Ocean Salinity (SMOS) mission [*Simmonds et al.*, 2004]. In this paper, a set of equations are proposed to retrieve emissivity as a function of SM at different spectral bands for six analyzed soil types.

[7] The paper proceeds as follows. The details of the experiment setup both for emissivity and SM measurements, as well as the soils description, are shown in section 2. The results and discussion of the experiment are analyzed in section 3. Finally, conclusions are given in section 4.

2. Experiment Setup

2.1. Soil Sample Descriptions

[8] A variety of samples of surface horizons (0–15 cm) of different soil types was selected for this experiment. The variation of TIR emissivity with SM was studied according to different soil textures (i.e., particle size). Parameters such as texture, porosity, structure, among others, are responsible of this variation.

[9] Each sample was characterized by its physical and chemical soil properties (Table 1) related to soil texture, color, organic matter content (OM), total carbonates, soil reaction (pH), electric conductivity (EC), cationic exchange capacity (CEC) and base saturation (V). The soil texture was determined according to the standard ISO 11277:1998 [*International Organization for Standardization*, 2002], based on sieving and sedimentation mechanical techniques.

[10] The taxonomic class of the soils and its diagnostic horizon were identified according to *Food and Agriculture Organization of the United Nations (FAO)* [1999] and soil taxonomy [*Natural Resources Conservation Service*, 1999] classifications (Table 1). The origin of each soil is specified in Table 1. Even though all the soils are from Spain, they are representative of Mediterranean areas, except sample E of Oceanic areas.
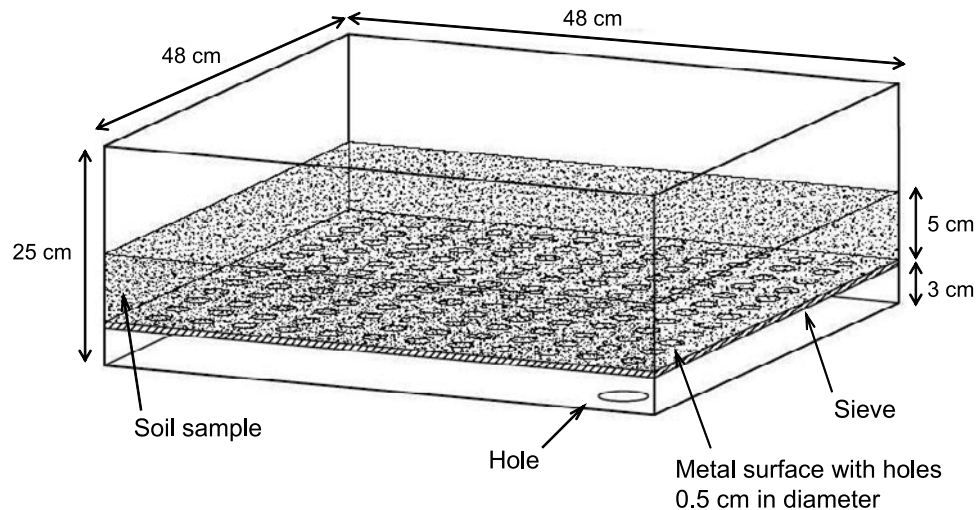
Figure 1.   Glass container with soil sample and water drainage system.

[11]   The identification of clay minerals of all samples was determined by means of the X-ray diffraction (XRD) technique and a semiquantitative analysis of the patterns (see Table 1) following the methods of *Warshall and Roy* [1961] and *Davis and Smith* [1989a, 1989b]. Quartz is the most abundant mineral on samples A, B and E, whereas calcite is the predominant mineral on samples C, D and F. The result is important since quartz contributes to increase the reflectance of the material between 7.7 and 9.7 μm and also near 12.6 μm, but with less intensity in this last case, and calcite causes an increase of the reflectance near 11.4 μm [*Rowan and Mars*, 2002], which means an emissivity decrease in those spectral regions. These characteristics will be more or less important depending on the quartz and calcite content of each sample.

2.2.   Soil Moisture Measurement

[12]   The first step in the measurement strategy was to grind and blend each sample after allowing it to be air dried, and then sieving it into 2 mm. In this way, a complete elimination of the possible impurities of the soil such as stones or leafs was carried out. Then, the soils were flooded allowing water filtration through the recipient that contains the soil. Since that moment it was freely dried.

[13]   A 48 × 48−cm^2 base and 25-cm height glass container (see Figure 1) was designed for allowing the water drainage and a practical execution of emissivity measurements. The sample was kept over a metal surface with holes 0.5 cm in diameter, which was elevated 3 cm upon the receptacle base. Moreover, a sieve was put on the metal surface to avoid the loss of the finest particles. A big hole at the receptacle base allowed us to eliminate the water of the container to make possible a complete and quick drying of the soils.

[14]   The gravimetric method was chosen for measuring the SM since this is the most accurate technique. It is a direct method based on the immediate determination of the soil water content [*Day*, 1965]. The main limitation is that it is a laborious and destructive method since small amounts of soil are removed from the total sample when SM measurements are done.

[15]   It is necessary to emphasize that the vapor exchange with the air above the sample must be considered since in TIR we are observing a skin effect. Capillary forces of a homogeneous sample are uniform, and thus there are no thermal anomalies under steady state. Those were the reasons why we were very careful in the soil moisture (SM) measurement process. Before and during each series of emissivity measurement, the whole sample was mixed in order to assure the homogeneity of its SM. Furthermore, the soil cracks appearing in the drying process were eliminated when necessary. Moreover, in order to consider the SM variations caused by vapor exchange with the air above the sample, we took at least three soil samples of 10 to 30 grams, one at the beginning of each series of emissivity measurements, another in the middle and the last at the end. Their average value together with the error was considered as the SM measurement. Soil samples were taken from several points as well as from the three first centimeters in depth. Besides, taking into account that the radiance observed by a TIR radiometer comes from the first micrometers of the surface soil layer in direct contact with the atmosphere, we can assume that the surface vertical gradient in volumetric SM is not an important parameter for this study.

[16]   Following the gravimetric method, SM is expressed by weight as the ratio of the mass of water present to the dry weight of the soil sample. Moreover, we express it by percentage, so that a SM greater than 100% means that the mass of water present into the wet soil is greater than the mass of the dry soil.

[17]   The masses were measured with a KERN 770 balance with an accuracy of $\pm 10^{-6}$ kg. Because of this high accuracy, the SM error was in general caused by the non ideal homogeneity of SM during the emissivity measurements.

2.3.   Emissivity Measurement

[18]   The emissivities were determined through the two-lid variant of the box method [*Rubio et al.*, 1997] and using a CIMEL CE-312 thermal infrared radiometer [*Legrand et al.*, 2000]. It has four spectral channels: one broad, 8−14 μm (channel 1), and three narrow channels, 8.2−9.2, 10.5−
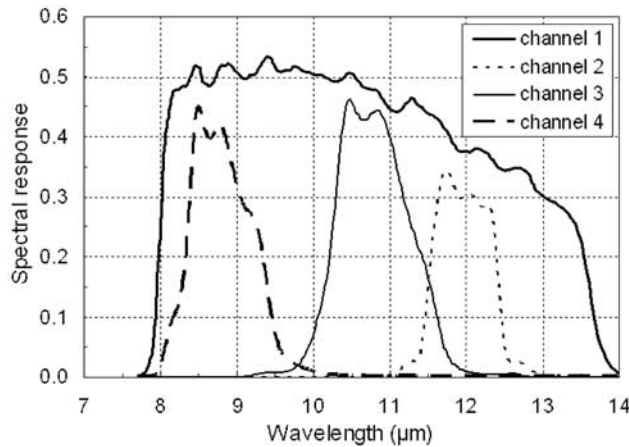
Figure 2. Relative spectral response of the high-precision multichannel thermal infrared radiometer CE-312.

11.5, 11.5–12.5 μm (channels 4, 3, and 2 respectively) as shown in Figure 2. The radiometer has a field of view of 10° and a response time of 1 s. A calibration of CE-312 with a Landcal Blackbody Source (Type P80P) within the temperature range −10 to 50°C was done during our experiment and accuracies of ±0.07, ±0.07, ±0.08 and ±0.09 K for channels 1 to 4, respectively, were obtained.

[19] The box is bottomless, with a base of 30×30 cm^2 and a height of 80 cm. The sidewalls are specular reflective surfaces of polished aluminum with an emissivity of $\varepsilon_c = 0.03$. Two interchangeable lids, each having a small central hole through which the radiometric measurements are taken, are used as a top. The "hot lid" is a cover of rough anodized aluminum painted in Parson's black with an emissivity value of $\varepsilon_h = 0.98$ kept at a temperature 15–20°C above the temperature of sample by means of an electric heating system. The "cold lid" is a specular reflective cover of polished aluminum, with an emissivity value of $\varepsilon_c = 0.03$.

[20] In the two-lid method, three measurements of radiance (L^1, L^2 and L^3) are performed with three different configurations of the box sample system. Moreover, a fourth measurement (L^4) was carried out in this work in order to quantify the effect of a nonideal box [see *Rubio et al.*, 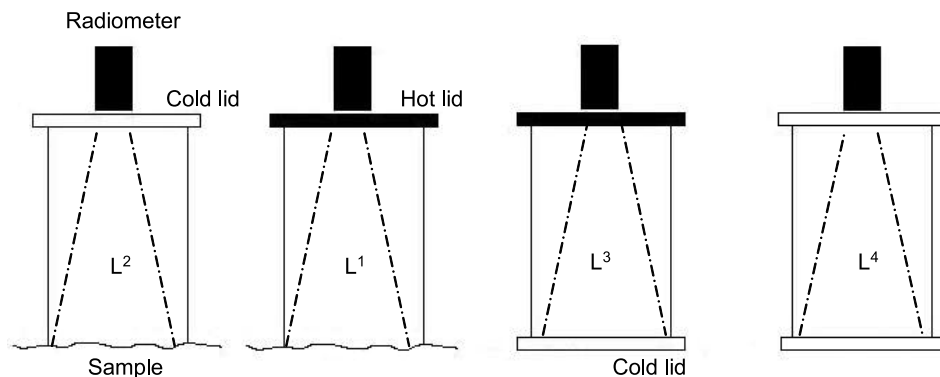1997]. This sequence of measurements is shown in Figure 3. In this way, the method gives the emissivity value of a ground sample as

$$\varepsilon = 1 - \frac{\left[L^1 - L^2\right]\left(1 - \varepsilon_c\right)}{\left(L^3 - L^2\right) - \left[L^3 - L^1\right]P + \left(L^2 - L^4\right)Q} \qquad (1)$$

where $P = 0.1460$ and $Q = 0.2921$ are factors which depend on the geometry of the box and the cold and hot lid emissivities.

[21] A series of 30 emissivity measurements per channel was carried out with the purpose of obtaining good statistics and reducing the error. In this way, only one average emissivity value was obtained from each series of measurements, which corresponds to a given SM value and spectral channel.

[22] It is important to emphasize that the sequence of soil saturation and drying were repeated at least two times in order to ensure the validity and reproducibility of emissivity measurements as well as for obtaining intermediate values of emissivity along the SM range.

3. Results and Discussion
3.1. Experimental Results

[23] The experimental results of the dependence of the TIR emissivity on SM at each spectral channel of CE-312 for each soil are shown in Figure 4. In relation to the SM, an exceptional value (1.17 kg kg^{-1}) of the highest SM value of the soil was obtained for calcic Kastanozem (sample C). The main cause of this high value was not only the wealth of organic matter content (OM) of this soil, but also its low bulk density (see Table 1). Table 1 shows that the OM content of sample C is four times the average OM content of the other samples. Although OM is generally a minor component of soils, it is the principal storage of plant available water because of the high percentage of water-stable aggregates. For this reason, soils with a high OM content have a different behavior than the others with regard to the retained water. Table 1 shows that bulk density of sample B is twice that of sample C, whereas the other samples have an intermediate bulk density. As results show, the highest SM value is higher for soils with lower bulk density.

Figure 3. Procedure followed for the emissivity measurement with the two-lid variant of the box method. The sequence of field measurements is from left to right (i.e., L^2, L^1, L^3, and L^4). Dashed lines represent the radiometer beam width.
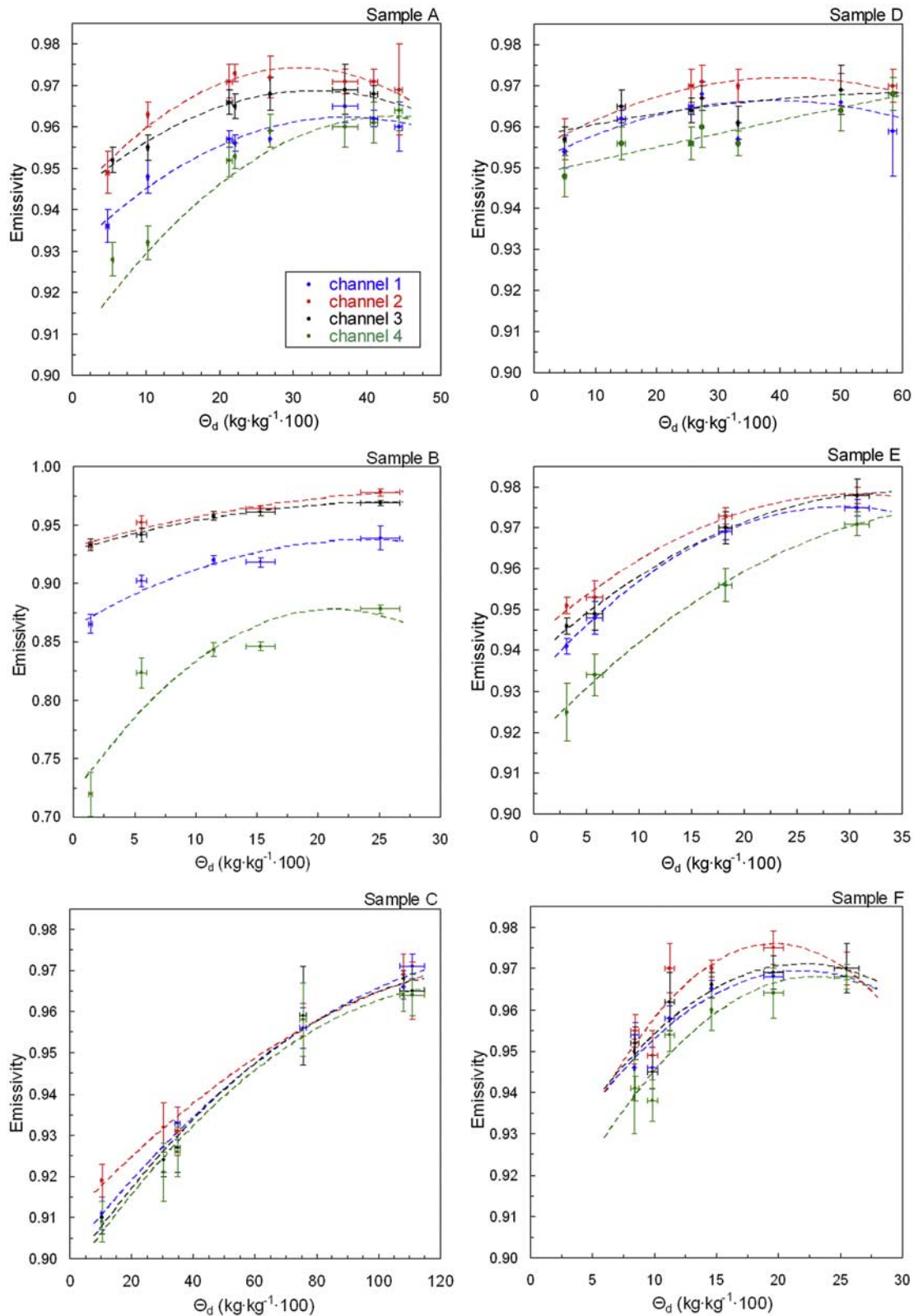
Figure 4. Measured emissivity of soils in the spectral channels of thermal infrared radiometer CE-312 for various moisture contents: channel 1, 8–14 μm; channel 2, 11.5–12.5 μm; channel 3, 10.5–11.5 μm; and channel 4, 8.2–9.2 μm. Dashed lines represent the fitting regression curves of emissivity against soil water content for each channel and sample, according to equation (2) and the coefficients given in Table 5.

Table 2. Maximum Emissivity Variation Within the Whole Soil Moisture Range, $\Delta\varepsilon_i$, and Its Error, $\delta(\Delta\varepsilon_i)$, and Average Emissivity Measurement Errors, $\overline{\delta\varepsilon_i}$, for Each Sample in the Different CE-312 Channels

Sample	$\Delta\varepsilon_1 \pm \delta(\Delta\varepsilon_1)$	$\Delta\varepsilon_2 \pm \delta(\Delta\varepsilon_2)$	$\Delta\varepsilon_3 \pm \delta(\Delta\varepsilon_3)$	$\Delta\varepsilon_4 \pm \delta(\Delta\varepsilon_4)$	$\overline{\delta\varepsilon_1}$	$\overline{\delta\varepsilon_2}$	$\overline{\delta\varepsilon_3}$	$\overline{\delta\varepsilon_4}$
A	0.029 ± 0.008	0.024 ± 0.007	0.017 ± 0.009	0.036 ± 0.009	0.003	0.005	0.004	0.004
B	0.074 ± 0.018	0.046 ± 0.007	0.036 ± 0.007	0.16 ± 0.02	0.006	0.004	0.004	0.009
C	0.060 ± 0.007	0.050 ± 0.009	0.058 ± 0.006	0.055 ± 0.010	0.004	0.005	0.006	0.006
D	0.031 ± 0.006	0.031 ± 0.009	0.029 ± 0.010	0.041 ± 0.011	0.004	0.004	0.004	0.005
E	0.034 ± 0.004	0.027 ± 0.006	0.032 ± 0.006	0.046 ± 0.010	0.003	0.004	0.004	0.005
F	0.023 ± 0.005	0.030 ± 0.008	0.028 ± 0.008	0.037 ± 0.007	0.003	0.005	0.004	0.005

[24] Except for sample C, the soils show a trend to increase their saturation point value with the increase (decrease) of clay (sand) content. Saturation point values were obtained in the laboratory [*Porta*, 1986] following the gravimetric method, with the purpose of checking this relationship. This is a consistent result since the soil matrix retains water by two mechanisms: first, water can be absorbed on particle surfaces (especially clay particles
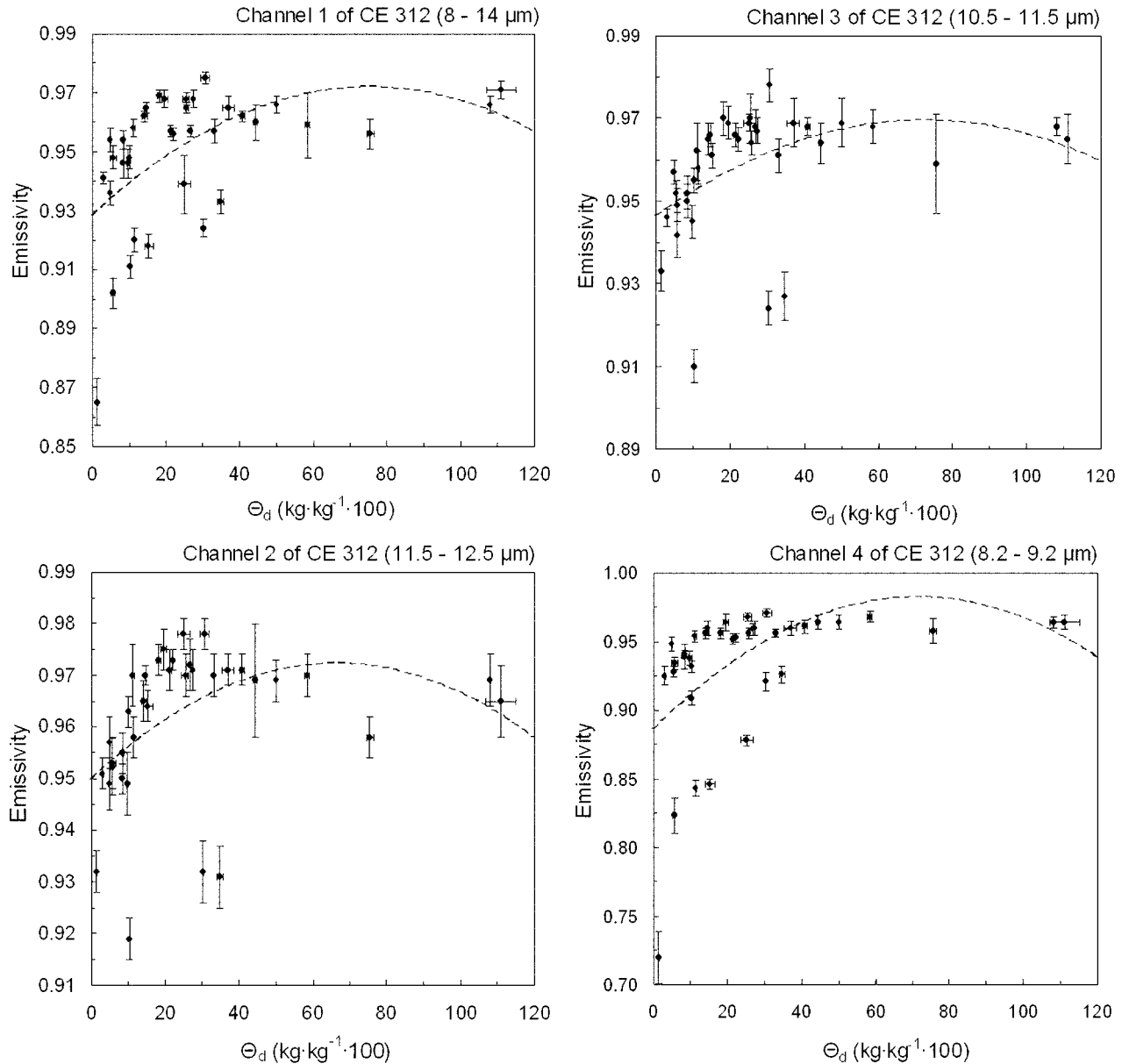

Figure 5. Emissivity measurements in the spectral channels of radiometer CE-312 for various moisture contents. Dashed lines represent the fitting regression curves of emissivity against soil water content for each channel, when all soils are considered together, according to equation (2) and the coefficients given in Table 3.

Table 3. Fitting Regression Curves of Emissivity, ε, Against Soil Water Content, Θ_d, for Each Channel Taking Into Account All Soils Together[a]

Channel	c	b	a	R^2	σ_f
		$\varepsilon = c \cdot \Theta_d^2 + b \cdot \Theta_d + a$			
1	−0.000008	0.0012	0.928	0.264	0.020
2	−0.000005	0.0007	0.950	0.178	0.013
3	−0.000004	0.0006	0.946	0.177	0.014
4	−0.000019	0.0027	0.886	0.257	0.045
		$\varepsilon = c \cdot P_s + b \cdot \Theta_d + a$			
1	−0.00036	0.00020	0.960	0.330	0.019
2	0.00008	0.00019	0.953	0.094	0.014
3	0.00008	0.00023	0.948	0.124	0.014
4	−0.00122	0.00017	0.983	0.493	0.037
		$\varepsilon_n = c \cdot \Theta_{dn}^2 + b \cdot \Theta_{dn} + a$			
1	−0.016	2.5	−2	0.729	18
2	−0.019	2.8	−1	0.680	21
3	−0.016	2.6	−2	0.739	19
4	−0.014	2.4	−2	0.822	15

[a]Sand content is also given in some cases; n: normalized value of the parameter; P_s: percentage of sand content of the soil; a, b and c: regression coefficients; R^2: determination coefficient; σ_f: fit standard error.

because of their reactive large surface area); and second, water can be held in soil pores by capillarity. It is a fact that water is held more tightly in smaller than in larger pores. For these reasons, clayey soils retain more water and for longer time than sandy soils.

[25] In relation to the emissivity behavior, an increase of emissivity with SM is observed in all cases. Table 2 compares the emissivity increase to the measurement errors, resulting that the increase is clearly larger than the experimental uncertainty. According to the values of Table 2, the mean error of emissivity is about ±0.5%. Note that the emissivity error is derived as the standard deviation of the set of 30 emissivity measurements taken each time. The highest variation of emissivity with SM is observed in the 8.2–9.2 μm in channel 4, followed by variations in channel 1 (8–13 μm), channel 2 (11.5–12.5 μm) and finally channel 3 (10.5–11.5 μm). The variability is more apparent in albic Arenosol, sample B ($\Delta \varepsilon_4 \sim 16\%$), and less marked in luvic Calcisol, sample A ($\Delta \varepsilon_3 \sim 1.7\%$).

[26] A large increase of emissivity for a low water content is generally observed in Figure 4, and then almost no changes are observed for moisture level above a certain SM value. According to Table 1, this SM value could coincide with the field capacity (FC) whose value depends on the soil type and generally is lower for soils with a higher sand content. A soil is at FC point when, after saturation, all water was drained from macropores by gravity. Then, micropores are able to hold water against the force of gravity by means of capillarity forces. This argument allows to understand the behavior of TIR emissivity in relation to SM since when soil is saturated, or even with a SM higher than its FC point, its thermal emissivity value is not only nearly constant but also close to one, similarly to the TIR emissivity of water. However, below the FC point, water is retained in micropores and macropores are full of air, allowing lower emissivity

values as well as a considerable emissivity variation with SM content and spectral region.

3.2. Parameterization

[27] In order to get a function for parameterizing the emissivity variation with SM, we first tried a unique relationship for all soil types at each spectral region. Figure 5 shows all the soil samples together for each channel. Different fitting curves were tested to adjust these points. First a quadratic fitting regression was used for each spectral channel:

$$\varepsilon_i = c_i \Theta_d^2 + b_i \Theta_d + a_i \qquad (2)$$

where a, b and c are the regression coefficients and the subindex i represents the CE-312 channel 1, 2, 3 or 4. The results are shown in Figure 5 and Table 3, in which we can see that low determination coefficients and high fit standard errors are obtained.

[28] Since the emissivity variation with SM depends on the sand or clay content, then we tried to obtain a fitting regression for bare soils taking into account both the SM and sand (or clay) content as follows:

$$\varepsilon_i = c_i P_s + b_i \Theta_d + a_i \qquad (3)$$

where P_s represents the percentage of sand content of the soil. The results were not good, as can be seen in Table 3, since the determination coefficients are lower than 0.5 for all channels. However, this was the expected result, since each sample has different properties that affect emissivity such as porosity, density, structure, among others. Therefore a common regression for all soils is difficult to be obtained if all these parameters are not considered.

[29] The results improve if both emissivity and SM are normalized using their maximum and minimum values according to the equations

$$\varepsilon_{in} = \frac{\varepsilon_i - (\varepsilon_i)_{min}}{(\varepsilon_i)_{max} - (\varepsilon_i)_{min}} \qquad (4)$$

$$\Theta_{dn} = \frac{\Theta_d - (\Theta_d)_{min}}{(\Theta_d)_{max} - (\Theta_d)_{min}} \qquad (5)$$

[30] The emissivity and SM of the air-dried soil were considered as $(\varepsilon_i)_{min}$ and $(\Theta_d)_{min}$, respectively, which correspond to the lowest values measured in the experiment. Meanwhile, the highest emissivity value $((\varepsilon_i)_{max})$ was considered as the average emissivity of the soil with a SM higher than its FC point, given in Table 1, because of the above mentioned invariance of the emissivity beyond this point. Nevertheless, only the maximum emissivity value was considered for sample C as $(\varepsilon_i)_{max}$ because of both the complex technique for getting its FC point and the particular behavior of emissivity with SM. Finally, the highest SM value $((\Theta_d)_{max})$ was considered as the saturation point of each soil, which was obtained in the laboratory [Porta, 1986]. All these values are collected in Table 4. As a result of a quadratic fitting regression such as equation (2) but considering normalized emissivity and SM values, the

Table 4. Minimum and Maximum Values of Emissivity and SM for Every Sample and Channel of Radiometer CE-312

Sample	$(\Theta_d)_{min}$, kg kg^{-1} 100	$(\Theta_d)_{max}$, kg kg^{-1} 100	$(\varepsilon_i)_{min}$	$(\varepsilon_i)_{max}$	Channel of CE-312
A	2.72 ± 0.02	60.4 ± 0.6	0.936 ± 0.004	0.961 ± 0.004	1
			0.949 ± 0.005	0.971 ± 0.006	2
			0.952 ± 0.003	0.967 ± 0.004	3
			0.928 ± 0.004	0.961 ± 0.005	4
B	0.029 ± 0.009	29.5 ± 0.6	0.865 ± 0.008	0.926 ± 0.006	1
			0.932 ± 0.004	0.967 ± 0.003	2
			0.933 ± 0.005	0.963 ± 0.003	3
			0.720 ± 0.019	0.856 ± 0.005	4
C	8.00 ± 0.05	117 ± 9	0.911 ± 0.004	0.971 ± 0.003	1
			0.919 ± 0.004	0.969 ± 0.005	2
			0.910 ± 0.004	0.968 ± 0.002	3
			0.909 ± 0.005	0.964 ± 0.004	4
D	2.60 ± 0.10	67.50 ± 0.05	0.941 ± 0.004	0.972 ± 0.002	1
			0.940 ± 0.005	0.971 ± 0.004	2
			0.940 ± 0.004	0.969 ± 0.006	3
			0.927 ± 0.007	0.968 ± 0.004	4
E	1.33 ± 0.04	40.4 ± 0.4	0.941 ± 0.002	0.972 ± 0.002	1
			0.951 ± 0.003	0.976 ± 0.003	2
			0.946 ± 0.002	0.974 ± 0.004	3
			0.925 ± 0.007	0.964 ± 0.004	4
F	0.920 ± 0.009	37.3 ± 1.7	0.945 ± 0.003	0.968 ± 0.003	1
			0.945 ± 0.004	0.973 ± 0.004	2
			0.942 ± 0.002	0.970 ± 0.005	3
			0.931 ± 0.004	0.966 ± 0.005	4

average determination coefficient improves four times (see Table 3) with respect to the nonnormalized one (R$^2 \sim 0.74$), but the results are not good enough in relation to the fit standard errors ($\sigma_f \sim 18\%$). The main drawback of this parameterization is the need of knowing both the TIR emissivity range and the water holding retention of the soils in study. However, this may not be a serious problem if it is possible to easily know these parameters since one can either work physically with the soils, in a laboratory or in the field, or obtain them by remote sensing measurements after a period of drought and an intense rain.

[31] Since it is not easy to find a unique function for all samples, we finally obtained regression curves for each soil separately. A quadratic fitting regression of emissivity against soil water content for each channel of CE-312 and sample (equation (2)) was derived with the best accuracy. In Table 5 the set of coefficients as well as the determination coefficients (R^2) and the fit standard errors (σ_f) are shown for every case. These parameterization curves, plotted in Figure 4, are much better since their average determination coefficient is around 0.90 and the fit standard error gets a value around ±0.5%. It is important to emphasize that sample D is the one which presents the worst adjustment. We think that this is due to the compacted texture that it got through the experiment, which made difficult the process of homogenizing soil water content, and the subsequent roughness reached. If this sample is not included, the determination coefficient increases to 0.95. Therefore the conclusion is that if a quadratic fitting regression of emissivity against soil water content for each channel and sample is considered, acceptable results are obtained.

3.3. Spectral Ratio

[32] An error of ±1 K in temperature causes about an error of about ±2% in emissivity and less than ±0.5% in emissivity ratios in the TIR. For this reason, *Urai et al.* [1997] proposed the emissivity ratio as a possible indicator of SM content. We analyzed the dependence of the spectral ratio between bands on the SM content of bare soils in two cases. First, the emissivity ratio between channel 4 (8.2–9.2 μm) and the average of channels 2 and 3 (10.5–12.5 μm), which is usually higher because of the presence of reststrahlen bands. Second, the ratio between channel 3 and channel 2, that corresponds to the classical split-window bands at 11 and 12 μm, respectively.

Table 5. Regression of Emissivity Against Soil Water Content for Each Channel and Sample[a]

		$\varepsilon_i = c_i \Theta_d^2 + b_i \Theta_d + a_i$				
Sample	Channel	$c \times 10^{-4}$, (kg kg^{-1} 100)$^{-2}$	$b \times 10^{-2}$, kg kg^{-1} 100	a	R^2	σ_f
A	1	−0.24	0.18	0.930	0.953	0.002
	2	−0.34	0.21	0.942	0.946	0.002
	3	−0.24	0.16	0.943	0.971	0.0013
	4	−0.29	0.24	0.914	0.978	0.002
B	1	−1.3	0.6	0.862	0.931	0.010
	2	−0.5	0.30	0.931	0.954	0.005
	3	−0.59	0.31	0.928	0.990	0.002
	4	−4	1.5	0.72	0.878	0.030
C	1	−0.031	0.10	0.901	0.991	0.003
	2	−0.025	0.08	0.910	0.986	0.003
	3	−0.04	0.11	0.897	0.988	0.003
	4	−0.04	0.11	0.895	0.985	0.004
D	1	−0.10	0.08	0.951	0.396	0.006
	2	−0.11	0.088	0.954	0.928	0.0016
	3	−0.03	0.03	0.957	0.586	0.003
	4	0.00	0.03	0.948	0.874	0.003
E	1	−0.50	0.291	0.9326	0.999	0.0003
	2	−0.38	0.23	0.943	0.989	0.002
	3	−0.34	0.23	0.938	0.995	0.0019
	4	−0.31	0.27	0.918	0.997	0.0019
F	1	−1.2	0.5	0.914	0.844	0.005
	2	−1.9	0.8	0.902	0.798	0.006
	3	−1.2	0.5	0.914	0.824	0.005
	4	−1.3	0.6	0.897	0.919	0.004

[a]R^2 is the determination coefficient; σ_f is fit standard error.

Table 6. Average Values of Emissivity for Channels 2 and 3 of Radiometer CE-312 for Each Sample, When Its Maximum Variation With SM is Considered

Sample	$\overline{\varepsilon_2}$	$\overline{\varepsilon_3}$
A	0.967	0.963
B	0.957	0.953
C	0.946	0.942
D	0.967	0.964
E	0.964	0.961
F	0.963	0.959

[33] In the first case, a total increase of emissivity ratio of 13% with moisture content is observed for sample B, because of the high spectral contrast related to the quartz reststrahlen band of sand. Similar to *Urai et al.* [1997], an increase about 3% in (8−9 μm)/(9.5−11.5 μm) ratio is shown for an increase of 2% in SM content. However, this increase is not linear as *Salisbury and D'Aria* [1992b] noted. The other samples present an average increase of the emissivity ratio of less than 3%. According to *Salisbury and D'Aria* [1992b], this fact is justified since soils that contain more than 1.5−2% extractable OM (see Table 1) tend to display low ASTER 10/14 ratios, {8.3 μm/11.3 μm}, since OM is highly absorbing in the 8−14 μm region and serves to reduce the apparent spectral contrast of the quartz reststrahlen bands. Nevertheless, in all cases, a reduction of the spectral contrast with moisture content is observed since water is very strongly absorbing in the region of the quartz reststrahlen bands. Taking into account the estimate error of the emissivity ratios, it seems that this quantity would be only useful as a SM indicator in the case of sandy soils.

[34] In the second case, no changes in the emissivity ratio are observed with respect to soil water content within the estimate errors of emissivity ratios. Therefore the emissivity ratio between channels 2 and 3 do not seem useful as a SM indicator, even for sandy soils.

3.4. Implications for LST Determination

[35] We also studied the implications for LST determination when the influence of SM on emissivity is not considered. Two cases were analyzed. First, the error of LST derived from a single-channel algorithm for atmospheric and emissivity correction [*Coll et al.*, 1994]. Second, the error in LST derived from a split-window algorithm for atmospheric and emissivity correction [*Coll and Caselles*, 1997].

[36] In relation to the first case studied, the emissivity correction derived from a single-channel algorithm can be written as [*Coll et al.*, 1994]

$$\Delta T_i = \frac{1 - \varepsilon_i}{\varepsilon_i} b_i \qquad (6)$$

where i is the channel considered and b_i is a coefficient which depends on surface temperature, atmospheric profile and spectral channel.

[37] In order to calculate the atmospheric parameters required for b_i, a simulation database was used. The database contains 234 clear-sky atmospheric profiles with a global distribution along all latitudes, and with a wide range not only of water vapor contents (from 0.015 to 7 cm), but also of surface temperatures (from −70 to +50°C). The

values of the atmospheric transmittance, the radiance at ground level and the downwelling atmospheric radiance, all of them at nadir observation angle, were simulated according to the database. The 11 μm and 12 μm Advanced Along Track Scanning Radiometer (AATSR)'s channels were chosen because of their similar spectral responses with channels 3 and 2 of CE-312, respectively. Only data relevant for this study are presented in this section and the reader is referred to *Galve et al.* [2006] for additional details on the simulation database.
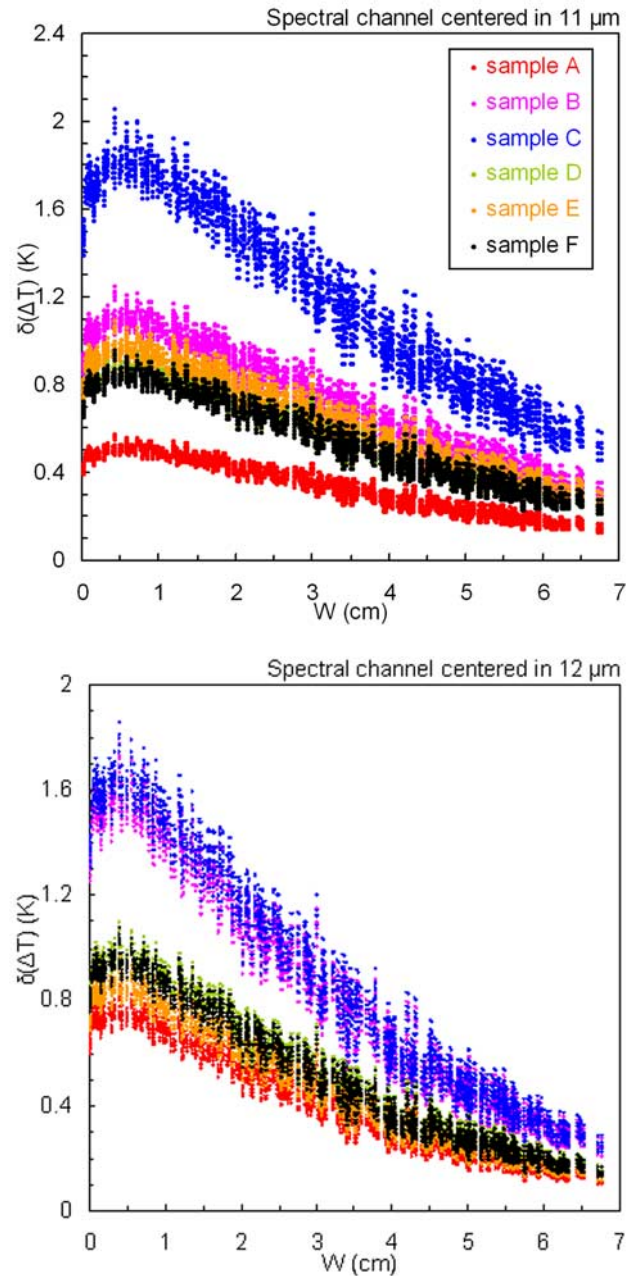

Figure 6. Error in LST ($\delta(\Delta T)$) derived from a single-channel algorithm for atmospheric and emissivity correction when soil moisture is not considered. (top) Channel centered at 11 μm and (bottom) channel centered at 12 μm. W is atmospheric water vapor content.
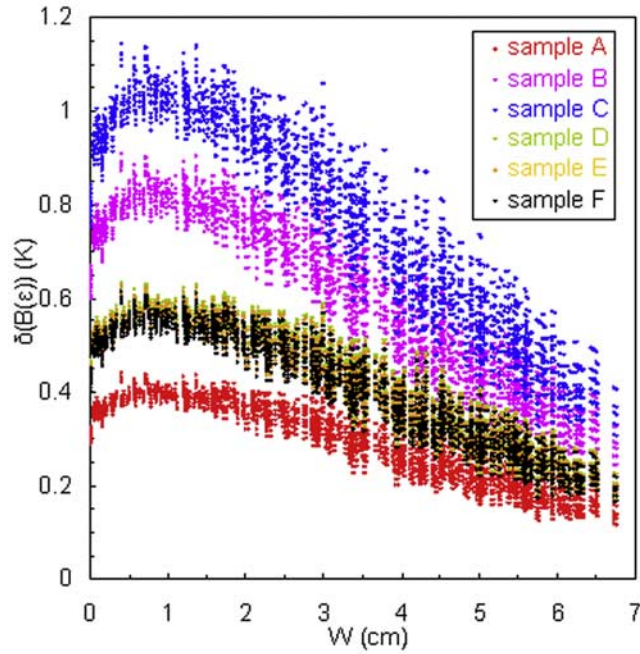
Figure 7. Error in LST [$\delta(\mathrm{B}(\varepsilon))$] derived from a split-window algorithm for atmospheric and emissivity correction when soil moisture is not considered. W is atmospheric water vapor content.

[38] The LST error caused by the fact of not considering SM can be written as

$$\delta(\Delta \mathrm{T_i}) = \frac{\Delta \varepsilon_i / 2}{\overline{\varepsilon}_i^2} \mathrm{b_i} \qquad (7)$$

where $\Delta \varepsilon_i / 2$ is the emissivity error, taken as half the variation of emissivity with SM content for each sample (from Table 2), and $\overline{\varepsilon_i}$ is the average value (see Table 6).

[39] This case is plotted in Figure 6, which shows a general decrease of error in LST with atmospheric water vapor content (or precipitable water, W). Considering all cases, the error can range between 0.1 K and 2 K, which can be significant in both channels. According to Figure 6, soils with a high OM content (as sample C) suffer the highest error in LST determination, and sample A shows the lowest impact, if the SM variation is not considered.

[40] In the second case, the error in LST derived from a split-window algorithm when SM is not considered, is analyzed. The split-window model of *Coll and Caselles* [1997] is used in this paper, in which the emissivity correction term can be written as

$$\mathrm{B}(\varepsilon) = \alpha(1 - \varepsilon) - \beta \Delta \varepsilon \qquad (8)$$

where $\varepsilon = (\varepsilon_i + \varepsilon_j)/2$ is the mean surface emissivity in two spectral channels (i and j), $\Delta \varepsilon = \varepsilon_i - \varepsilon_j$ is the spectral emissivity difference in these channels, and coefficients α and β depend on the atmospheric properties and were calculated from the simulated data.

[41] According to observations of previous section, the contribution of the second term of equation (8) is negligible,

since the emissivity spectral ratio between channels 3 and 2 of CE-312 shows a negligible variation with SM. However, the impact of the first term in the emissivity effect is not negligible because of the values of the above mentioned terms, $\Delta \varepsilon_i / 2$, which have a direct influence on the error of the mean emissivity, ε, considered this time. The error in $\mathrm{B}(\varepsilon)$ is

$$\delta(\mathrm{B}(\varepsilon)) = \alpha \frac{\sqrt{(\Delta \varepsilon_i / 2)^2 + (\Delta \varepsilon_j / 2)^2}}{2} \qquad (9)$$

[42] This error is shown in Figure 7 for all samples. This time, the term $\sqrt{(\Delta \varepsilon_3 / 2)^2 + (\Delta \varepsilon_2 / 2)^2}/2$ is the direct responsible of the high or low value of $\delta(\mathrm{B}(\varepsilon))$. In comparison with single-channel algorithm, the impact in the emissivity effect is lower, but not negligible. In general, a LST error from 0.1 K to 1.1 K is common for all bare soils. In consequence, the SM content of bare soils should be considered to avoid significant systematic errors in the LST determination.

4. Conclusions

[43] This paper stresses the importance of an accurate determination of emissivity variation with soil water content to permit suitable temperature retrievals, not only for sandy soils which have the greatest variation, but also for a variety of soils with different soil texture.

[44] A set of six mineral soils was used as a basis for studying the dependence of the TIR emissivity on SM from laboratory measurements. Each soil has a different soil texture, and therefore different emissivity behaviors were observed. However, a general trend to increase the emissivity with soil water content is common for every soil studied. We think that the increase is caused by the water film on the soil particles decreasing its reflectivity. The results show that emissivity increase is larger in the 8.2–9.2 μm range than in the 10.5–11.5 μm range, following the sequence $\Delta \varepsilon_4(8.2–9.2 \ \mu\mathrm{m}) > \Delta \varepsilon_1(8–13 \ \mu\mathrm{m}) > \Delta \varepsilon_2(11.5–12.5 \ \mu\mathrm{m}) \sim \Delta \varepsilon_3(10.5–11.5 \ \mu\mathrm{m})$ accordingly to previous studies [*Salisbury and D'Aria*, 1992b; *Urai et al.*, 1997; *Xiao et al.*, 2003]. Moreover, this variation is higher for larger sand content in a soil. Considering both the quartz contribution to decrease the emissivity of the material chiefly between 7.7 and 9.7 μm (spectral range included in channel 4), and the emissivity value close to one of water in TIR, the large increase of emissivity when soil water content increases can be understood. The variation of emissivity with SM is more obvious for albic Arenosol (sample B) with an increase by about 16% in channel 4 because it is the soil with a higher sand content. These variations are significant since they are clearly larger than the experimental uncertainty ($\delta \varepsilon \sim \pm 0.5\%$), and can involve an important impact in the current methods of temperature estimation from radiometric data.

[45] After showing that a general curve fit for all soils is not adequate to model emissivity variation with SM, even normalizing emissivity and SM, a quadratic fitting regression of emissivity against soil water content for each channel and sample was derived which can be useful in atmospheric and emissivity correction algorithms.

[46] The study shows that the spectral ratio decreases with increasing SM. The emissivity ratio of channel 4 and the average of channels 2 and 3 was proposed to be an indicator of this dependence [*Urai et al.*, 1997]. Albic Arenosol suffers the highest variation of this emissivity ratio (an increase of about 13% with increase in SM), whereas the other samples present an increase of the average emissivity ratio by less than 3%. Meanwhile, in the case of the classical split-window channels (channels 2 and 3 of CE-312), this contrast is almost constant.

[47] The implications for LST determination when SM is not considered is analyzed by means of two methods. First, the error in LST derived from a single-channel algorithm for atmospheric and emissivity correction, and second, from a split-window algorithm. The results show that systematic errors from 0.1 K to 2 K can be caused by SM influence on emissivity.

[48] To sum up, this study proves that the emissivity variation with SM should be considered in atmospheric and emissivity correction algorithms to avoid significant land surface temperature systematic errors.

References

Alex, Z. C., and J. Behari (1998), Laboratory evaluation of emissivity of soils, *Int. J. Remote Sens.*, 19(7), 1335–1340.

Burke, E. J., and L. P. Simmonds (2003), Effects of sub-pixel heterogeneity on the retrieval of soil moisture from passive microwave radiometry, *Int. J. Remote Sens.*, 24(10), 2085–2104.

Chen, J. M., B. J. Yang, and R. H. Zhang (1989), Soil thermal emissivity as affected by its water content and surface treatment, *Soil Sci.*, 148(6), 433–435.

Coll, C., and V. Caselles (1997), A split-window algorithm for land surface temperature from advanced very high resuolution radiometer data: Validation and algorithm comparison, *J. Geophys. Res.*, 102(14), 16,697–16,713.

Coll, C., V. Caselles, J. A. Sobrino, and E. Valor (1994), On the atmospheric dependence of the split-window equation for land surface temperature, *Int. J. Remote Sens.*, 15, 105–122.

Davis, B. L., and D. Smith (1989a), Table of experimental reference intensity ratios, *Powder Diffr.*, 3, 201–205.

Davis, B. L., and D. Smith (1989b), Table of experimental reference intensity ratios. Table n° 2, *Powder Diffr.*, 4, 206–209.

Day, P. R. (1965), Particle fractionation and particle-size analysis, in *Methods of Soil Analysis*, vol. 1, *Physical and Mineralogical Properties, Including Statistics of Measurement and Sampling, Agronomy*, vol. 9, edited by C. A. Black et al., pp. 545–567, Am. Soc. of Agron., Madison, Wis.

Food and Agriculture Organization of the United Nations (FAO) (1999), *World Reference Base for Soil Resources*, 90 pp., Rome.

Galantowicz, J. F., D. Entekhabi, and E. G. Njoku (2000), Estimation of soil-type heterogeneity effects in the retrieval of soil moisture from radiobrightness, *IEEE Trans. Geosci. Remote Sens.*, 38, 312–316.

Galve, J. M., C. Coll, V. Caselles, E. Valor, R. Niclòs, J. M. Sánchez, and M. Mira (2006), Simulation and validation of land surface temperature algorithms for MODIS and AATSR data, paper presented at 2nd International Symposium on Recent Advances in Quantitative Remote Sensing, Univ. de Valencia, Torrent, Spain.

International Organization for Standardization (2002), Soil quality. Determination of particle size distribution in mineral soil material. Method by sieving and sedimentation, *Rep. ISO 11277:1998/TC190*, Geneva, Switzerland, 30 pp.

Jackson, T. J., D. M. Le Vine, A. Y. Hsu, A. Oldark, P. J. Starks, C. T. Swift, J. D. Isham, and M. Haken (1999), Soil moisture mapping at regional scales using microwave radiometry: The southern great plains hydrology experiment, *IEEE Trans. Geosci. Remote Sens.*, 37, 2136–2151.

Legrand, M., C. Pietras, G. Brogniez, M. Haeffelin, N. K. Abuhassan, and M. Sicard (2000), A high-accuracy multiwavelength radiometer for in situ measurements in the thermal infrared: Part 1. Characterization of the instrument, *J. Atmos. Oceanic Technol.*, 17, 1203–1214.

Natural Resources Conservation Service (1999), Soil taxonomy. A basic system of soil classification for making and interpreting soil surveys, *Agric. Handbook 436*, 870 pp., Soil Surv. Staff, U.S. Dep. of Agric., Washington, D. C.

Ogawa, K., T. Schmugge, and S. Rokugawa (2006), Observations of the dependence of the thermal infrared emissivity on soil moisture, *Geophys. Res. Abstr.*, 8, 04996.

Porta, J. (1986), *Técnicas y Experimentos en Edafología*, 282 pp., Coll. Oficial d'Eng. Agron. de Catalunya, Barcelona, Spain.

Rowan, L. C., and J. C. Mars (2002), Lithologic mapping in the Mountain Pass, California area using Advanced Spaceborne Thermal Emission and Reflection radiometer (ASTER) data, *Remote Sens. Environ.*, 84, 350–366.

Rubio, E., V. Caselles, and C. Badenas (1997), Emissivity measurements of several soils and vegetation types in the 8–14 μm wave band: Analysis of two field methods, *Remote Sens. Environ.*, 59, 490–521.

Salisbury, J. W., and D. M. D'Aria (1992a), Emissivity of terrestrial materials in the 8–14 μm atmospheric window, *Remote Sens. Environ.*, 42, 83–106.

Salisbury, J. W., and D. M. D'Aria (1992b), Infrared (8–14 μm) remote sensing of soil particle size, *Remote Sens. Environ.*, 42, 157–165.

Saxton, K. E., W. J. Rawls, J. S. Romberger, and R. I. Papendick (1986), Estimating generalized soil-water characteristics from texture, *Soil Sci. Soc. Am. J.*, 50(4), 1031–1036.

Simmonds, L. P., et al. (2004), Soil moisture retrieval by a future spaceborne Earth observation mission, *Eur. Space Agency Study Rep.*, 14662/00/NL.

Soriano, M. D., and V. Pons (2001), *Prácticas de Edafología y Climatología*, 140 pp., Univ. Politec. de Valencia, Valencia, Spain.

Urai, M., T. Matsunaga, and T. Ishii (1997), Relationship between soil moisture content and thermal infrared emissivity of the sand sampled in Muus Desert, China, *Remote Sens. Soc. Jpn.*, 17(4), 322–331.

Van Bavel, C. H. M., and D. Hillel (1976), Calculating potential and actual evaporation from a bare soil surface by simulation of concurrent flow of water and heat, *Agric. Meteorol.*, 17, 453–476.

Warshall, C., and R. Roy (1961), Classification and scheme for the identification of layer silicates, *Geol. Soc. Am. Bull.*, 72, 1455–1492.

Xiao, Q., Q. H. Liu, X. W. Li, L. F. Chen, Q. Liu, and X. Z. Xin (2003), A field measurement method of spectral emissivity and research on the feature of soil thermal infrared emissivity, *J. Infrared Millimeter Waves*, 22(5), 373–378.

R. Boluda, Department of Vegetal Biology, Faculty of Pharmacy, University of Valencia, Av. Vicent Andrés Estellés, S-N, E-46100 Burjassot, Spain.

V. Caselles, C. Coll, M. Mira, and E. Valor, Department of Earth Physics and Thermodynamics, Faculty of Physics, University of Valencia, 50 Dr. Moliner, E-46100 Burjassot, Spain. (maria.mira@uv.es)